Efficient Cobalt Catalyzed Coupling of Amines and Siloxanes to Prepare Ceramics and Polymers

Anuja Sharma, † Ren H. Bean, † Timothy E. Long, † and Ryan J. Trovitch †, *

[†]School of Molecular Sciences and Biodesign Center for Sustainable Macromolecular Materials and Manufacturing, Arizona State University, Tempe, Arizona 85287, United States.

*Email: ryan.trovitch@asu.edu; Phone: 480-727-8930

KEYWORDS

Waste Prevention, Atom Economy, Less Hazardous Synthesis, Catalysis, Earth-Abundant Metals, Main Group Elements, Copolymers

ABSTRACT

The phosphine-substituted aryl diimine cobalt catalyst, (Ph2PPrADI)Co, has been found to mediate the dehydrocoupling of diamines or polyamines to poly(methylhydrosiloxane) (PMHS) to generate hydrogen and crosslinked solids in an atom-efficient fashion. The resulting siloxane diamine and siloxane polyamine networks persist in the presence of air or water at room temperature and can tolerate temperatures of up to 1,600 °C. Upon lowering the catalyst loading to 0.01 mol%, (Ph2PPrADI)Co was found to catalyze the dehydrocoupling of 1,3-propanediamine and PMHS (m = 35) to generate a siloxane diamine foam with a turnover frequency of 157 s⁻¹ relative to diamine consumption, the highest activity ever reported for Si–N dehydrocoupling. Furthermore, upon systematically reducing the number of potential branch points, the (Ph2PPrADI)Co catalyzed dehydrocoupling of diamines with hydride-terminated poly(dimethylsiloxane) (PDMS) was found to yield linear siloxane diamine polymers with molecular weights of up to 47,300 g/mol.

INTRODUCTION

Silicon nitride (Si₃N₄) and silicon oxynitride (SiO_xN_y) materials and coatings offer exceptional structural stability at temperatures of up to 1,400 °C.^{1,2} Raw Si₃N₄ powder is produced following

the reaction of N₂ with Si and textured using hot-press and sintering techniques.³⁻⁵ Chemical vapor deposition (CVD) using SiCl₄/NH₃, SiH₄/NH₃, or aminosilane monomers offers a route to Si₃N₄ coatings.⁵⁻⁷ The pyrolysis of preceramic polymers is a third methodology that generates Si₃N₄ and SiO_xN_y ceramics.⁸⁻¹⁰ Polysilazanes, which feature a repeating backbone of Si–N bonds, have been used as preceramic polymers for more than four decades to coat semiconductors and building materials.^{11,12} However, they are largely accessed through the ammonolysis or aminolysis of halosilanes (Figure 1, a).¹³ The corrosive nature of halosilanes and generation of an equivalent of ammonium salt waste for each Si–N bond that is formed are major drawbacks of this approach. These factors have inspired researchers to prepare polysilazanes, and ultimately Si₃N₄, in an atom-efficient fashion by dehydrocoupling amines and silanes (Figure 1, b).¹⁴⁻¹⁶

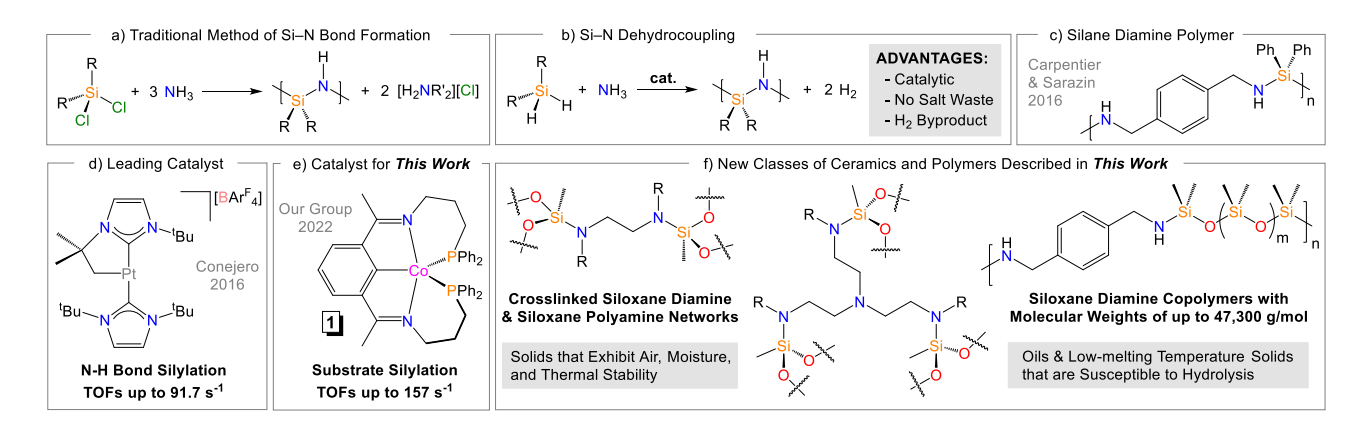


Figure 1. Strategy for the Co-catalyzed synthesis of siloxane-based networks and linear polymers *via* Si–N dehydrocoupling.

Polymers that possess alternating silane and diamine moieties (Figure 1, c) have been described in recent Si–N dehydrocoupling efforts, $^{17\text{-}20}$ including examples derived from SiH₄. 21 Although they have been referred to in the literature as polycarbosilazanes, compounds of this type may more appropriately be thought of as silane diamine copolymers since they lack the C–Si–N backbones that genuine polycarbosilazanes feature. 22,23 The ceramic uses of silane diamine copolymers or branched materials have not been widely explored; however, ferrocene-based examples were recently found to yield magnetic materials that feature α -Fe and α -Fe₂O₃ upon pyrolysis. 19

It must also be mentioned that a significant number of main group, $^{24-39}$ transition metal, $^{20,40-51}$ and f-block element $^{52-58}$ catalysts have been found to mediate the heterodehydrocoupling of amines and silanes to prepare aminosilane monomers. 59 The most active catalyst for Si–N dehydrocoupling reported to date by a significant margin is $[Pt(I'Bu')(I'Bu)][BAr^F_4]$, (I'Bu = 1,3-di-t-butylimidazolylidene; I'Bu' = the corresponding t-butyl activated metallacycle; Figure 1, d). 49 This catalyst was found to mediate Si–N dehydrocoupling with turnover frequencies (TOFs) of up to 330,000 h⁻¹, more accurately expressed as 5,500 min⁻¹ since the trials were conducted over minutes instead of hours, and as 91.7 s^{-1} for the purpose of this contribution.

Despite the considerable amount of effort that has gone into developing catalysts from across the periodic table, cobalt catalysts have never been used for the dehydrocoupling of amines and silanes. Recently, we described the synthesis and characterization of (Ph2PPTADI)Co (1, Figure 1, e), which features a Co(I) center and a redox innocent pentadentate aryl diimine (ADI) ligand. 60 This complex was found to mediate carbonyl hydrosilylation with TOFs of up to 330 s⁻¹ at ambient temperature, the highest ever reported for this transformation. This underlying activity led us to evaluate its activity for related reactions, including the silylation of N–H bonds. Herein, this transformation is used for the first time to prepare crosslinked siloxane diamine and polyamine solids that exhibit exceptional thermal stability, as well as linear diamine siloxane oils, by tailoring the siloxane that is used (Figure 1, f). In the process, 1 has been found to mediate Si–N dehydrocoupling with ambient temperature TOFs of up to 157 s⁻¹ on a per substrate basis, the highest ever reported for this transformation.

RESULTS AND DISCUSSION

Siloxane Diamine Network Synthesis and Characterization. This study was initiated with the addition of diamines and trimethylsilyl-terminated PMHS featuring an average of 35 Si–H bonds per oligomer to 1 (Table 1). For example, ethylenediamine was added to PMHS so that an equal ratio of N–H and Si–H bonds were present. Then, this mixture was added to a benzene- d_6 solution featuring 0.2 M mesitylene as an internal standard and 0.5 mol% of 1 relative to diamine. The reaction bubbled vigorously due to the evolution of H₂ and a solid formed within seconds. The trial was allowed to sit at room temperature for 5 min to promote additional crosslinking, and was then exposed to air to deactivate the catalyst. The residual solution was analyzed by ¹H NMR spectroscopy and free ethylenediamine was not observed, indicating that

this substrate was fully consumed (>99% conv.). The precipitate was collected by vacuum filtration, washed with toluene, and dried to afford a white solid (1a) that is insoluble in aprotic organic solvents including THF, CHCl₃, and CH₂Cl₂.

Table 1. Preparation of siloxane diamine networks through the dehydrocoupling of diamines and polyamines with PMHS (m = 35) using 0.5 mol% 1.^a

^a All substrates are >99% dehydrocoupled in 5 min as judged by ¹H NMR integration of starting amines against mesitylene as the internal standard. Isolated yields of the siloxane diamine solids are provided in parenthesis. ^b Diamine was dissolved in 3 mL THF.

The substrate scope was initially expanded to include diamines that feature longer carbon chains. Using the same procedure, the 1 catalyzed dehydrocoupling of PMHS (m = 35) to 1,3propanediamine allowed for >99% substrate utilization to afford 1b in 88% yield. For longer chain diamines that are solids at room temperature, 3 mL of THF was added. Even at lower concentrations (neat diamine in PMHS vs. 0.3 M diamine in a THF solution of PMHS), 1,4butanediamine, 1,6-hexanediamine, and 1,12-dodecanediamine dehydrocoupling resulted in vigorous bubbling and the formation of solids 1c-1e within seconds. Fourier-transform infrared spectroscopy (FT-IR) proved particularly useful for elucidating differences in composition and crosslink density. For example, each compound was found to exhibit a characteristic Si-N stretch at 835-875 cm⁻¹. However, the FT-IR analysis of **1a** revealed the presence of an N-H stretch at 3,426 cm⁻¹ along with a Si-H stretch at 2,169 cm⁻¹ (Figure S1). The presence of both peaks suggests that Si–N dehydrocoupling within 1a is incomplete, which may be attributed to the inability of its short ethylenediamine linkers to access additional siloxane Si-H moieties following their incorporation. As diamine chain length is extended, the intensity of N-H and Si-H stretching deceases to the point where these peaks are no longer visible. For example, the spectrum of **1d** was found to exhibit C–H (2,967 cm⁻¹), Si–O (1,013 cm⁻¹) and Si–N (845 cm⁻¹) stretches with a strong C-H bending mode at 746 cm⁻¹. Given the lack of apparent N-H and Si-H stretching, the structure of 1d must largely feature tertiary amine environments (where the R group in Table 1 is siloxane).

To further expand the substrate scope, 0.5 mol% of 1 was found to couple diamines possessing ether functionalities to PMHS (m = 35), yielding 1f and 1g within 5 min (Table 1, R = H and siloxane). The dehydrocoupling of 1,4-bis(aminomethyl)benzene and PMHS (m = 35) afforded a beige, rather than white, solid in 94% yield (1h). The isolation of a THF insoluble siloxane diamine solid derived from 1,4-bis(aminomethyl)benzene is noteworthy since this substrate has largely been dehydrocoupled to silanes to prepare soluble oligomers and polymers. To provide further evidence that 1 is capable of generating tertiary aminosilanes, the coupling of *N*,*N*'-dimethyl-1,3-propanediamine with PHMS (m = 35) was performed. Although the instantaneous solidification observed for primary amine entries in Table 1 did not occur, product 1i began to precipitate from solution after approximately 1 min as a bright yellow solid. Finally, the scope was extended to include the polyamines diethylenetriamine and tris(2-aminoethyl)amine. Products 1j and 1k were obtained as off-white solids that did not feature an

infrared N–H stretching vibration, indicating the presence of tertiary amine linkages and a high degree of crosslinking. Product **1k** has a higher crosslink density than other products in Table 1 since dehydrocoupling occurs at three primary amines, and IR spectroscopic analysis suggests that **1a**, **1f**, and **1h** feature the lowest crosslink density of the products derived from unsubstituted diamines.

Network Stability. Several experiments were then performed to evaluate the stability of the siloxane diamine covalent networks in Table 1. First, a sample of 1d was analyzed by IR spectroscopy immediately after being removed from inert atmosphere. The remainder of the sample was exposed to air featuring 15-25% humidity, and IR data was collected over the course of 1 week at ambient temperature (Figure S14). Notably, no changes were noted, suggesting that the Si–N bonds of 1d resist hydrolysis due to the tertiary amine environments and high degree of crosslinking present. To determine if less crosslinked materials exhibit the same stability, this experiment was repeated for 1a, 1f, and 1h. No IR changes were noted after 1 week, indicating that hydrolytic stability is a general feature of the products in Table 1. Not all networks featuring Si–N bonds exhibit this behavior. For example, we recently reported that the products of SiH4 and diamine dehydrocoupling decompose after 1 h in air.²¹ In some cases, they were even found to combust upon H₂O addition. The difference in reactivity between these materials stems from the underlying stability of the silane environments that are present (i.e., the aminated siloxane moieties in 1a-1k are far less reactive than the diamino- and triaminosilane linkages obtained from SiH4 dehydrocoupling).

Next, the thermogravimetric analysis (TGA) of each product was performed. For 1a, the temperature at which 5% of its initial weight was lost ($T_{d5\%}$) was determined to be 419 °C (Table 2, entry 1). The most significant weight loss for this compound was approximately 30%, with an inflection point (T_{inf}) of 558 °C. Upon extending the diamine carbon chain length, even higher $T_{d5\%}$ (597 °C) and T_{inf} (622 °C) values were observed for 1c. Remarkably, this product loses only 15% of its weight upon heating to 900 °C. However, as the distance between the Si–N linkages continues to increase, the relative stability of 1d-1g decreases (TGA analysis of 1d-1f revealed two inflection points, the first being at relatively low temperature). The product derived from 1,4-bis(aminomethyl)benzene (1h) was particularly resistant to weight loss upon heating, with $T_{d5\%} = 638$ °C and $T_{inf} = 755$ °C. The product of secondary amine dehydrocoupling (1i) was

found to exhibit $T_{d5\%} = 540$ °C and $T_{inf} = 673$ °C, suggesting that the chain length between the Si–N bonds is a key predictor of siloxane diamine weight loss. However, the degree of crosslinking also minimizes volatile compound release upon heating given that the product of tris(2-aminoethyl)amine dehydrocoupling (1k) exhibited a $T_{d5\%} = 744$ °C and a total weight loss of only 7% at 900 °C (even though this compound has a 27% carbon content). Unsurprisingly, differential scanning calorimetry (DSC) analysis on each crosslinked network did not reveal definitive glass transition temperatures (T_g) between -50 and 175 °C (1a-1k, see SI).

Table 2. TGA of crosslinked siloxane diamine networks **1a-1k**.^a

Entry	Product	Td5%	T_{Dinf}	Percent Weight
Entry	Froduct	(°C)	(°C) (°C)	Loss at 900 °C
1	1a	419	558	39%
2	1b	469	510	45%
3	1c	597	622	15%
4	1d	225	95, 622	18%
5	1e	173	158, 604	21%
6	1f	90	116, 572	45%
7	1g	131	144	34%
8	1h	638	755	10%
9	1i	540	673	13%
10	1j	456	456	17%
11	1k	744	650, 746	7%

^a Determined from 25 °C to 900 °C with a ramp rate of 10 °C/min under N₂ flow.

The weight loss values reported for **1a-1k** upon heating to 900 °C give rise to ceramic yields that range from 55-93%, with the highest yields observed for **1k** (93%), **1h** (90%), and **1i** (87%). To gain insight into the ceramics being formed, a sample of **1b** was heated at 1,000 °C for 2 h and powder X-ray diffraction analysis revealed that the material remained amorphous. Heating a second sample of **1b** to 1,400 °C for the same amount of time also yielded an amorphous product; however, pyrolysis at 1,600 °C for 2 h under argon resulted in a 47% yield of SiO₂ (Figure S40). Repeating this experiment under N₂ afforded a 7% yield of Si₃N₄, present as a mixture of Si₃N₄-159 and Si₃N₄-173 (Figure 2, a). The lack of Si₃N₄ formed under argon, and low yield of it obtained under nitrogen, are due to Si₃N₄ dissociation into silicon and nitrogen at 1,600 °C. ⁶¹ Moreover, the conversion of Si₃N₄-159 to Si₃N₄-173 is well-documented at elevated temperatures. ⁶²

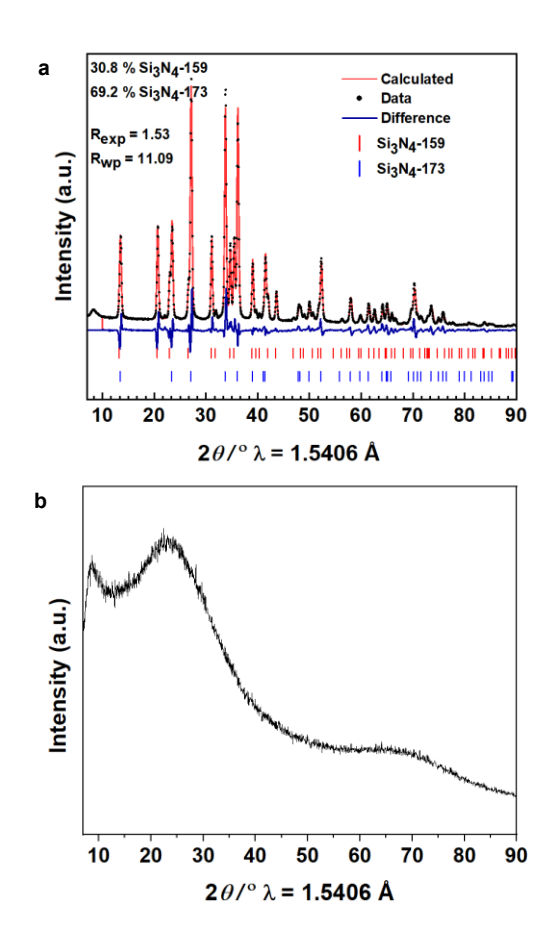


Figure 2. a) Powder XRD data collected upon heating **1b** to 1,600 °C for 2 h under N₂. b) Powder XRD data collected upon heating **1k** to 1,600 °C for 2 h under Ar.

To our surprise, subjecting highly crosslinked **1k** to 1,600 °C for 2 h under argon returned an amorphous ceramic in 79% yield, as judged by powder X-ray diffraction (Figure 2, b). This experiment suggests that these newly developed siloxane polyamine network solids are promising materials for extreme environments. It should be mentioned that the closest compounds to **1a-1k** prepared via Si–N dehydrocoupling are NH-bridged hydrosiloxane cyclomers described by Laine and co-workers.⁶³

Maximizing Si–N Dehydrocoupling Activity. For each entry in Table 1, dehydrocoupling proceeded with a TOF of 39.6 min⁻¹ based on diamine silylation (i.e., 198 equiv. of diamine were consumed per equiv. of **1** over the course of 5 min). However, this does not account for the true Si–N dehydrocoupling activity of the catalyst since crosslinked materials are being obtained. For example, in the process of synthesizing **1a**, at least two N–H bonds must be dehydrocoupled to

generate a solid, suggesting that **1** performed Si–N dehydrocoupling with a TOF of at least 79.2 min⁻¹. To determine this TOF experimentally, an ethylenediamine and PMHS mixture was sealed in a thick-walled glass bomb and a THF solution featuring 0.5 mol% of **1** was isolated in the arm of the bomb under N₂ with a septum. A stopwatch was initiated upon opening the bomb valve and mixing the solutions, and after 5 min, the septum was punctured with a hose-fitted needle to allow for collection and measurement of the generated hydrogen in an upside-down graduated cylinder filled with water. This procedure revealed that 2.2 N–H bonds per ethylenediamine were silylated, equating to a Si–N dehydrocoupling TOF of 87.1 min⁻¹. Repeating this procedure revealed the dehydrocoupling of 2.3 N–H bonds per 1,3-diaminopropane equivalent (TOF = 91.1 min⁻¹) and 3.3 N–H bonds per tris(2-aminoethyl)amine equivalent (TOF = 130.7 min⁻¹).

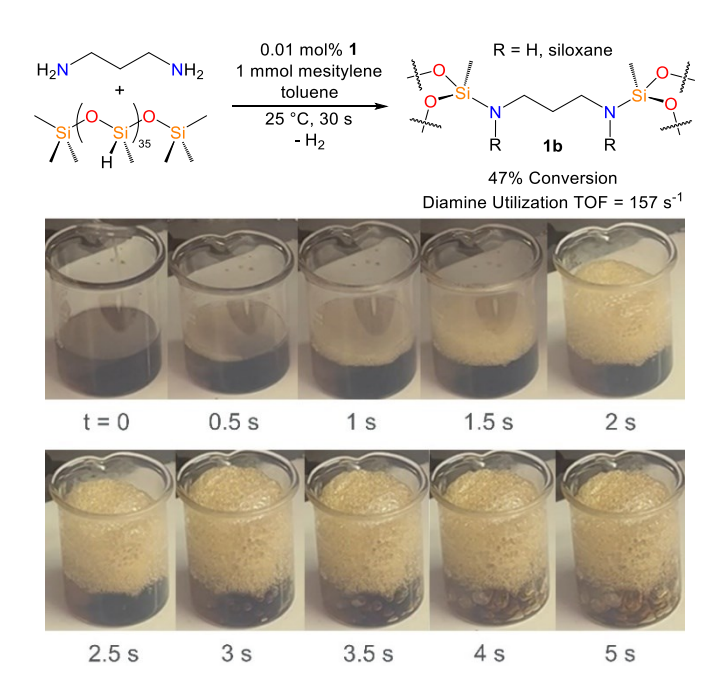


Figure 3. Time-resolved formation of siloxane diamine foam 1b using 0.01 mol% 1.

To determine the maximum observable TOF of 1-mediated Si–N dehydrocoupling, 1,3-propanediamine and PMHS (m = 35) in 5.0 mL toluene featuring mesitylene as an internal standard was added to 0.01 mol% of 1. The reaction was rapid and it resulted in the formation of a high modulus siloxane diamine foam within 5 s (Figure 3). Crosslinking was allowed to continue, and after 30 s, an aliquot of the residual solution was added to a vial containing iodine to quench the catalyst. The 1 H NMR spectrum of this solution in benzene- d_6 revealed 47%

consumption of 1,3-propanediamine relative to the mesitylene standard, equating to a substrate conversion TOF of 157 s⁻¹. As described earlier, network formation requires the formation of two or more Si–N bonds per diamine, equating to an Si–N dehydrocoupling TOF of *at least* 314 s⁻¹. This estimated value represents an average TOF over the course of 30 s,⁶⁴ and is far below the maximum TOF of 1-catalyzed Si–N dehydrocoupling given that foam formation was observed and largely complete within 5 s (a process that may also prevent complete substrate utilization). This foam did not degrade upon floating in ambient temperature water over the course of 7 days (Figure S9), indicating that it may be a suitable insulation material.⁶⁵

Role of Siloxane Chain Length. With an understanding of how 1 catalyzes the formation of highly crosslinked siloxane diamine solids, soluble copolymers were sought. First, the PMHS was modified so that the average chain possessed 38 (2,485 g/mol), 30 (1,950 g/mol), or 24 (1,600 g/mol) hydride functionalities. In the presence of 0.5 mol% 1, these siloxanes were quickly dehydrocoupled to 1,3-diaminopropane to generate solids 2a-2c (Figure 4, a), which exhibit physical, spectral, and thermal properties that are similar to 1b. Since the IR spectrum of 2c was found to feature a weak N–H stretching vibration at 3,339 cm⁻¹ (Figure S52), a further reduction in the number of potential crosslink points was pursued. Notably, adding 1 to a solution of 1,3-diaminopropane and PMHS (m = 4; 390 g/mol) did not result in solid formation. With a 1.0 mol% catalyst loading, these reagents were dehydrocoupled over the course of 4 h to yield 2d as an oil (Figure 4, b). This trial required a higher catalyst loading and an extended reaction time of 4 h to reach completion, and the product was found to be crosslinked by IR spectroscopy (Figure S58).

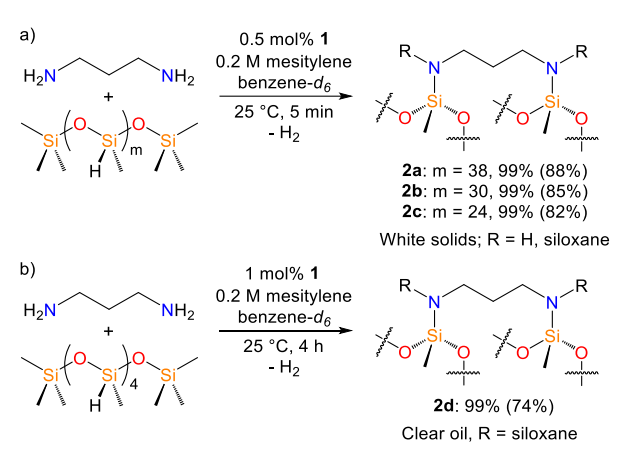


Figure 4. a) Formation of covalent networks 2a-2c. b) Reducing the number of PHMS branch points to obtain siloxane diamine oil 2d.

Linear Siloxane Diamine Copolymers. To evaluate whether 1-catalyzed siloxane diamine copolymer synthesis could be extended to the formation of linear products, the dehydrocoupling of diamines with hydride-terminated siloxanes was pursued (Table 3). Using a 1 mol% loading of 1 in benzene- d_6 solution, the coupling of 1,3-propanediamine to 1,1,3,3-tetramethyldisiloxane was found to reach completion within 5 h at ambient temperature. The corresponding product, 3a, was isolated as an oil in 85% yield and found to feature a ¹H NMR spectrum consistent with linear polymer formation (Figure S59). Integration revealed two NH protons per diamine equivalent, a small quantity of excess disiloxane, and evidence for hydrosiloxane end groups, indicating that 3a is a minimally-branched alternating copolymer.

Table 3. Formation of siloxane diamine copolymers from 1,3-propanediamine and hydrideterminated siloxanes of different length using 1 mol% 1.^a

^a All substrates are >99% dehydrocoupled in 5 h as judged by ¹H NMR integration of starting reagents. Isolated yields of the siloxane diamine polymers are provided in parenthesis.

Next, the 1-mediated dehydrocoupling of 1,3-propanediamine with a hydride-terminated poly(dimethylsiloxane) (PDMS) featuring an average of 4 D-groups per chain (m = 4) was evaluated under the same conditions. Greater than 99% diamine conversion to linear polymer 3b was observed by ¹H NMR spectroscopy over the course of 5 h, and the ²⁹Si NMR spectrum of this product was found to feature resonances for the expected hydrosiloxane, siloxazane (O-Si-N), and siloxane environments at -6.85, -10.97, and -21.83 ppm, respectively (Figure S69). Lastly, the 1-catalyzed dehydrocoupling of 1,3-propanediamine and hydride-terminated PDMS (m = 12) afforded siloxane diamine copolymer 3c in 93% yield under the same conditions. Analysis of 3a and 3b by MALDI-TOF mass spectrometry revealed masses consistent with the fragmentation of each polymer, with Gaussian distributions observed at weights of up to 3,000 g/mol (Figure S62 and S70). An analogous, but weaker intensity pattern, was observed for 3c due to the greater distribution of monomers present in the PDMS (m = 12) substrate. Upon evaluating the ¹³C NMR spectra of 3a-3c, a mixture of products was apparent in the case of 3a and 3c, but not for 3b. Compound 3b was also the most robust of the products, with less than 20% weight loss observed at temperatures of up to 450 °C. Therefore, hydride-terminated PDMS (m = 4) was chosen as the preferred dehydrocoupling partner to evaluate the scope of 1-catalyzed linear siloxane diamine formation.

Dehydrocoupling using an equimolar ratio of this siloxane and an assortment of diamines was then conducted in the presence of 1 mol% 1 in benzene- d_6 (Table 4). The complete consumption of each diamine was observed after 5 h at ambient temperature, and the respective linear siloxane diamine polymers 4a-4h were obtained in moderate to high yields (61-98%). Each of these products was found to exhibit a relatively simple ¹H NMR spectrum consistent with the presence of two NH protons per diamine equivalent, and a new ²⁹Si NMR resonance between -9 and -12 ppm due to the formation of siloxazane linkages. The 1-mediated dehydrocoupling of ether- (4f, 4g) and aryl-substituted (4h) diamines proceeded seamlessly to afford linear siloxane diamine copolymers. Compounds 4c, 4d, 4e and 4h were obtained as solids, while other products in Table 3 were obtained as oils. With the exception of 4f, the products were found to feature a ²⁹Si NMR resonance consistent with the presence of hydrosiloxane end groups, rendering them interesting telechelic polymers for further polymerization.

Table 4. Dehydrogenative coupling of diamines with hydride-terminated PDMS (m = 4) using 1 mol% 1.^a

Diamine + Si
$$\begin{pmatrix} 1 & mol \% & 1 & benzene-d_6 \\ \hline 25 ° C, 5 & h & -H_2 & -H_2 & -H_3 & -H_4 &$$

^a All substrates are >99% dehydrocoupled in 5 h as judged by ¹H NMR integration of starting reagents. Isolated yields of the siloxane diamine polymers are provided in parenthesis.

The moisture stability of a representative solution of **4b** in benzene-*d*₆ was then evaluated. After 10 min of exposure to air featuring 23% humidity, a large quantity of free diamine was observed by ¹H NMR spectroscopy. Moreover, NMR tubes featuring solutions of **4a-4h** were found to develop acid and base resistant coatings upon prolonged exposure to air, due to polymer hydrolysis and siloxane functionalization of the glass surface. Because of their moisture sensitivity, the molecular weights of **4a-4h** could not be determined using gel permeation chromatography. However, the solubility of these products did allow for estimation of their molecular weight (M_w) via diffusion ordered NMR spectroscopy (DOSY). The diffusion coefficients for **4a-4h** were determined by NMR signal attenuation over a range of pulsed field gradient strengths and were found to vary from 0.62-1.85 x 10⁻¹⁰ m²/s (Table 5). The hydrodynamic radii of these polymers was then calculated using the Stokes-Einstein equation, and the diffusion coefficient-molecular weight method described by Grubbs and co-workers⁶⁶ afforded an estimation of M_w for each product (Table 5). Polymer **4h** was found to possess the lowest diffusion coefficient (0.66 x 10⁻¹⁰ m²/s) and highest molecular weight (47,300 g/mol).

Product **4e** was found to have a higher M_w (42,100 g/mol) than **4a-4d**, which may be due to the length of its dodecane diamine units. The M_w of **4f** was the lowest of the products analyzed (6,200 g/mol), which is likely related to the fact that this product was not found to feature Si–H end groups by ¹H and ²⁹Si NMR spectroscopy. MALDI-TOF mass spectrometry data was also collected for **4a-4h**. Unsurprisingly, this method revealed polymer fragments with regularly spaced Gaussian mass distributions, and the highest molecular weight fragments (of up to 7,100 g/mol) were observed for the product with the lowest diffusion coefficient, **4h**.

Table 5. Polymer properties determined by ¹H DOSY NMR spectroscopy.

Product	Diffusion	Hydrodynamic	M_{w}
	coefficient	Radius ^a	$(g/mol)^b$
	$(10^{-10} \text{ m}^2/\text{s})$	(Å)	
4a	0.89	40	24,100
4b	1.09	33	18,100
4c	1.15	42	15,000
4d	0.89	40	24,100
4e	0.66	54	42,100
4f	1.85	19	6,200
4g	1.17	30	14,500
4h	0.62	57	47,300

^a Hydrodynamic radius calculated from the Stokes-Einstein equation. ^b Molecular weight estimated by ¹H DOSY NMR spectroscopy in benzene- d_6 at 25 °C using the polystyrene standard calibration curve reported by Grubbs. ⁶⁶

In general, TGA of **4a-4h** revealed that these linear polymers release volatile compounds at lower temperatures than their highly crosslinked counterparts, **1a-1h**. Notably, the loss of weight from **4a-4h** was dependent on diamine chain length. For example, **4a** and **4b** were found to lose approximately 20% of their initial weight upon heating to 450 °C. Extending the diamine chain length to four carbons in **4c** led to 20% weight loss upon heating to 350 °C, while **4d** and **4e** lost approximately 20% percent of their weight upon heating to 300 °C and 200 °C, respectively. Ether-functionalized polymers **4f** and **4g** significantly degrade before heating to 200 °C, while **4h** was found to exhibit comparable weight loss to **4d**.

The difference in moisture stability observed between crosslinked materials **1a-1k** and their linear counterparts **4a-4h** also warrants mention. By building considerable crosslink density into

PMHS-derived diamine or polyamine networks, it was possible to synthesize preceramic materials that do not degrade upon extended exposure to air or water. In contrast, upon coupling hydride-terminal PDMS to diamines, linear polymers that are highly susceptible to hydrolysis were obtained. Although Si–N bonds are far easier to hydrolyse than functional groups commonly employed in chemically recyclable or biodegradable polymers, ^{67,68} they can be surprisingly robust within a crosslinked hydrophobic matrix.

CONCLUSIONS

The (Ph₂PPr</sup>ADI)Co-catalyzed coupling of diamines and polyamines with trimethylsilyl-terminated PMHS (m = 35) afforded covalent networks that are persistent at temperatures of up to 1,600 °C. These reactions, representing the first reported examples of cobalt-based Si–N dehydrocoupling, were found to proceed with substrate utilization TOFs of 40 min⁻¹. Lowering the loading of (Ph₂PPr ADI)Co to 0.01 mol% allowed for Si–N dehydrocoupling with a TOF of 157 s⁻¹ based on 1,3-propanediamine consumption, and an N–H bond silylation TOF of at least 314 s⁻¹, representing the highest activity that has ever been reported for this transformation. By reducing the number of hydride equivalents present on the poly(siloxane) coupling partner, siloxane diamine oils were preferentially synthesized. Extension of this methodology to the dehydrocoupling of diamines and hydride-terminated siloxanes afforded linear siloxane diamine copolymers with molecular weights of up to 47,300 g/mol.

ASSOCIATED CONTENT

Supporting Information. The Supporting Information is available free of charge at http://pubs.acs.org.

General considerations, detailed experimental procedures, product images, and characterization data (¹H, ¹³C, ²⁹Si, and DOSY NMR, IR, TGA, DSC, XRD, and MALDI-TOF MS). (PDF)

AUTHOR INFORMATION

Corresponding Author

Ryan J. Trovitch – School of Molecular Sciences and Biodesign Center for Sustainable Macromolecular Materials and Manufacturing, Arizona State University, Tempe, Arizona

85287, United States; ORCID: 0000-0003-4935-6780; Phone: (480) 727-8930; Email: ryan.trovitch@asu.edu

Authors

Anuja Sharma – School of Molecular Sciences and Biodesign Center for Sustainable Macromolecular Materials and Manufacturing, Arizona State University, Tempe, Arizona 85287, United States; ORCID: 0000-0001-8563-8457

Ren H. Bean – School of Molecular Sciences and Biodesign Center for Sustainable Macromolecular Materials and Manufacturing, Arizona State University, Tempe, Arizona 85287, United States

Timothy E. Long – School of Molecular Sciences and Biodesign Center for Sustainable Macromolecular Materials and Manufacturing, Arizona State University, Tempe, Arizona 85287, United States

Author Contributions

The manuscript was written through contributions of all authors. All authors have given approval to the final version of the manuscript.

Notes

A. S. and R. J. T. retain rights to 1, and the formation of siloxane diamine ceramics and polymers via dehydrocoupling, through U.S. Patent Application No. 63/249,151.

ACKNOWLEDGMENTS

This material is based upon work supported by the National Science Foundation under Grant No. 2154359. Prof. Christina S. Birkel and Mr. Jordan Sinclair are acknowledged for assisting with powder X-ray diffraction analysis. We would also like to thank Prof. Richard M. Laine for helpful discussions.

REFERENCES

1. Ziegler, G., Heinrich, J.; Wötting, G. Relationships between processing, microstructure and properties of dense and reaction-bonded silicon nitride. *J. Mater. Sci.* **1987**, *22*, 3041-3086. DOI: 10.1007/BF01161167

- 2. Ryall, W. R.; Muan, A. Silicon Oxynitride Stability. *Science*, **1969**, *165*, 1363-1364. DOI: 10.1126/science.165.3900.1363
- 3. Zhu, X.; Sakka, Y. Textured silicon nitride: processing and anisotropic properties. *Sci. Technol. Adv. Mater.* **2008**, *9*, 033001. DOI: 10.1088/1468-6996/9/3/033001
- 4. Jiang, Q.-G.; Liu, J.; Liu, W.-M.; Cheng, L. X.; Gong, M.-F.; Wu, S.-H. A Novel Hot Pressing Flowing Sintering for Preparation of Texturing Ceramics. *J. Am. Ceram. Soc.* **2015**, *98*, 2696-2699. DOI: 10.1111/jace.13715
- 5. Kroke, E.; Schwarz, M. Novel group 14 nitrides, *Coord. Chem. Rev.* **2004**, *248*, 493-532. DOI: 10.1016/j.ccr.2004.02.001
- 6. Kaloyeros, A. E.; Jové, F. A.; Goff, J.; Arkles, B. Review—Silicon Nitride and Silicon Nitride-Rich Thin Film Technologies: Trends in Deposition Techniques and Related Applications. *ECS J. Solid State Sci. Technol.* **2017**, *6*, P691-P714. DOI: 10.1149/2.0011710jss 7. Kaloyeros, A. E.; Pan, Y.; Goff, J.; Arkles, B. Review—Silicon Nitride and Silicon Nitride-Rich Thin Film Technologies: State-of-the-Art Processing Technologies, Properties, and Applications. *ECS J. Solid State Sci. Technol.* **2020**, *9*, 063006. DOI: 10.1149/2162-8777/aba447
- 8. Blum, Y. D.; Schwartz, K. B.; Laine, R. M. Preceramic polymer pyrolysis. *J. Mater. Sci.*, **1989**, *24*, 1707-1718. DOI: 10.1007/BF01105695
- 9. Birot, M.; Pillot, J. P.; Dunogues, J. Comprehensive Chemistry of Polycarbosilanes, Polysilazanes, and Polycarbosilazanes as Precursors of Ceramics. *Chem. Rev.*, **1995**, *95*, 1443-1477. DOI: 10.1021/cr00037a014
- 10. Ackley, B. J.; Martin, K. L.; Key, T. S.; Clarkson, C. M.; Bowen, J. J.; Posey, N. D.; Ponder Jr., J. F.; Apostolov, Z. D.; Cinibulk, M. K.; Pruyn, T. L.; Dickerson, M. B. Advances in the Synthesis of Preceramic Polymers for the Formation of Silicon-Based and Ultrahigh-Temperature Non-Oxide Ceramics. *Chem. Rev.* **2023**, *123*, 4188-4236. DOI: 10.1021/acs.chemrev.2c00381
- 11. Riedel, R.; Seher, M.; Mayer, J.; Szabó, D. V. Polymer-derived Si-based bulk ceramics, part I: Preparation, processing and properties. *J. Eur. Ceram. Sci.*, **1995**, *15*, 703-715. DOI: 10.1016/0955-2219(95)00041-R
- 12. Jeon, K. S.; Joo, K. C.; Shin, W. S.; Yun, K. H. Annealing Process of Polysilizane Layer and Method of Forming Isolation Layer of Semiconductor Device Employing the Same. U.S. Pat. Appl. **2008**, US 2008/0194074 A1.

- 13. Laine, R. M.; Blum, Y. D.; Tse, D.; Glaser, R. Synthetic Routes to Oligosilazanes and Polysilazanes. *ACS Symp. Ser.* **1988**, *360*, 124-142. DOI: 10.1021/bk-1988-0360.ch010
- 14. Blum, Y. D.; Laine, R. M. Catalytic methods for the synthesis of oligosilazanes.
- Organometallics, 1986, 5, 2081-2086. DOI: 10.1021/om00141a026
- 15. Liu, H. Q.; Harrod, J. F. Copper(I)-catalyzed cross-dehydrocoupling reactions of silanes and amines. *Can. J. Chem.*, **1992**, *70*, 107-110. DOI: 10.1139/v92-018
- 16. Seyferth, D.; Stewart, R. M. Synthesis and polymerization of cyclotetrasilazanes. *Appl. Organomet. Chem.*, **1997**, *11*, 813–832. DOI: 10.1002/(SICI)1099-
- 0739(199710/11)11:10/11<813::AID-AOC641>3.0.CO;2-%23
- 17. Bellini, C.; Orione, C.; Carpentier, J.; Sarazin, Y. Tailored Cyclic and Linear Polycarbosilazanes by Barium-Catalyzed N–H/H–Si Dehydrocoupling Reactions. *Angew. Chem. Int. Ed.*, **2016**, *55*, 3744-3748. DOI: 10.1002/anie.201511342
- 18. Bellini, C.; Roisnel, T.; Carpentier, J.; Tobisch, S.; Sarazin, Y. Sequential Barium-Catalysed N–H/H–Si Dehydrogenative Cross-Couplings: Cyclodisilazanes versus Linear Oligosilazanes. *Chem. Eur. J.*, **2016**, 22, 15733-15743. DOI: 10.1002/chem.201603191
- 19. Morris, L. J.; Whittell, G. R.; Eloi, J. C.; Mahon, M. F.; Marken, F.; Manners, I.; Hill, M. S. Ferrocene-Containing Polycarbosilazanes via the Alkaline-Earth-Catalyzed Dehydrocoupling of Silanes and Amines. *Organometallics*, **2019**, *38*, 3629-3648. DOI:
- 10.1021/acs.organomet.9b00444
- 20. Gasperini, D.; King, A. K.; Coles, N. T.; Mahon, M. F.; Webster, R. L. Seeking Heteroatom-Rich Compounds: Synthetic and Mechanistic Studies into Iron Catalyzed Dehydrocoupling of Silanes. *ACS Catal.*, **2020**, *10*, 6102-6112. DOI: 10.1021/acscatal.0c01440
- 21. Nguyen, T. T.; Mukhopadhyay, T. K.; MacMillan, S. N.; Janicke, M. T.; Trovitch, R. J. Synthesis of Aminosilane Chemical Vapor Deposition Precursors and Polycarbosilazanes through Manganese-Catalyzed Si–N Dehydrocoupling. *ACS Sustainable Chem. Eng.* **2022**, *10*, 4218-4226. DOI: 10.1021/acssuschemeng.2c00008
- 22. Zhang, G.-B.; Fan, X.-D.; Kong, J.; Liu, Y.-Y.; Wang, M.-C.; Qi, Z.-C. Structure Design of Novel Hyperbranched Polycarbosilazanes: Synthesis and Characterization. *Macromol. Chem. Phys.* **2007**, *208*, 541-548. DOI: 10.1002/macp.200600482
- 23. Veith, M.; Elsässer, R.; Krüger, R.-P. Synthesis of Dendrimers with a N–Si–C Framework. *Organometallics*, **1999**, *18*, 656-661. DOI: 10.1021/om9807708

- 24. Corriu, R. J. P.; Leclercq, D.; Mutin, P. H.; Planeix, J. M.; Vioux, A. Silicon-nitrogen bond formation by nucleophilic activation of silicon-hydrogen bonds, *J. Organomet. Chem.*, **1991**, 406, C1-C4. DOI: 10.1016/0022-328X(91)83192-7
- 25. Buch F.; Harder, S. The Azametallacyclopropane Ca(η²-Ph₂CNPh)(hmpa)₃: A Calcium Alternative to a Versatile Ytterbium(II) Catalyst. *Organometallics*, **2007**, *26*, 5132-5135. DOI: 10.1021/om700626s
- 26. Dunne, J. F.; Neal, S. R.; Engelkemier, J.; Ellern, A.; Sadow, A. D. Tris(oxazolinyl)boratomagnesium-catalyzed cross-dehydrocoupling of organosilanes with amines, hydrazine, and ammonia. *J. Am. Chem. Soc.*, **2011**, *133*, 16782-16785. DOI: 10.1021/ja207641b
- 27. Hill, M. S.; Liptrot, D. J.; MacDougall, D. J.; Mahon, M. F.; Robinson, T. P. Heterodehydrocoupling of silanes and amines by heavier alkaline earth catalysis. *Chem. Sci.*, **2013**, *4*, 4212-4222. DOI: 10.1039/C3SC51797G
- 28. Greb, L.; Tamke, S.; Paradies, J. Catalytic metal-free Si–N cross-dehydrocoupling. *Chem Commun.*, **2014**, *50*, 2318-2320. DOI: 10.1039/C3CC49558B
- 29. Pérez, M.; Caputo, C. B.; Dobrovetsky, R.; Stephan, D. W. Metal-free transfer hydrogenation of olefins via dehydrocoupling catalysis. *P. Natl. Acad. Sci. USA*, **2014**, *111*, 10917-10921. DOI: 10.1073/pnas.1407484111
- 30. Allen, L. K.; Garcia-Rodriguez, R.; Wright, D. S. Stoichiometric and catalytic Si–N bond formation using the p-block base Al(NMe₂)₃. *Dalton Trans.*, **2015**, *44*, 12112-12118. DOI: 10.1039/C5DT00662G
- 31. Bellini, C.; Carpentier, J.; Tobisch, S.; Sarazin, Y. Barium-Mediated Cross-Dehydrocoupling of Hydrosilanes with Amines: A Theoretical and Experimental Approach. *Angew. Chem. Int. Ed.*, **2015**, *54*, 7679-7683. DOI: 10.1002/anie.201502956
- 32. Bellini, C.; Dorcet, V.; Carpentier, J.; Tobisch, S.; Sarazin, Y. Alkaline-Earth-Catalysed Cross-Dehydrocoupling of Amines and Hydrosilanes: Reactivity Trends, Scope and Mechanism. *Chem. Eur. J.*, **2016**, *22*, 4564-4583. DOI: 10.1002/chem.201504316
- 33. Anga, S.; Sarazin, Y.; Carpentier, J.; Panda, T. K. Alkali-Metal-Catalyzed Cross-Dehydrogenative Couplings of Hydrosilanes with Amines. *ChemCatChem*, **2016**, *8*, 1373-1378. DOI: 10.1039/C6RA04125F

- 34. Baishya, A.; Peddarao, T.; Nembenna, S. Organomagnesium amide catalyzed cross-dehydrocoupling of organosilanes with amines. *Dalton Trans.*, **2017**, *46*, 5880-5887. DOI: 10.1039/C7DT00806F
- 35. Forosenko, N. V.; Basalov, I. V.; Cherkasov, A. V.; Fukin, G. K.; Shubina, E. S.; Trifonov, A. A. Amido Ca(II) complexes supported by Schiff base ligands for catalytic cross-dehydrogenative coupling of amines with silanes. *Dalton Trans.*, **2018**, 47, 12570-12581. DOI: 10.1039/c8dt01130c
- 36. Li, N.; Guan, B. A Dialkyl Calcium Carbene Adduct: Synthesis, Structure, and Catalytic Cross-Dehydrocoupling of Silanes with Amines. *Eur. J. Inorg. Chem.*, **2019**, 2231-2235. DOI: 10.1002/ejic.201900168
- 37. Rauch, M.; Roberts, R. C.; Parkin, G. Reactivity of [Tism^{PriBenz}]MgMe towards secondary amines and terminal alkynes: Catalytic dehydrocoupling with hydrosilanes to afford Si–N and Si–C bonds. *Inorganic Chimica Acta*, **2019**, 494, 271-279. DOI: 10.1016/j.ica.2019.03.015 38. Palumbo, F.; Rohrbach, S.; Tuttle, T.; Murphy, J. A. N-Silylation of Amines Mediated by Et₃SiH/KO^rBu. *Helv. Chim. Acta*, **2019**, *102*, e1900235. DOI: 10.1002/hlca.201900235 39. Wirtz, L.; Lambert, J.; Morgenstern, B.; Schäfer, A. Cross-Dehydrocoupling of Amines and Silanes Catalyzed by Magnesocenophanes. *Organometallics*, **2021**, *40*, 2108-2117. DOI: 10.1021/acs.organomet.1c00245
- 40. Saam, J. C.; Speier, J. L. Preparation of 3-Triethoxysilylpropylamine and 1,3-Bis(3-aminopropyl)tetramethyldisiloxane. *J. Org. Chem.*, **1959**, *24*, 119-120. DOI: 10.1021/jo01083a612
- 41. Sommer, L. H.; Citron, J. D.; Group VIII metal-catalyzed reactions of organosilicon hydrides with amines, hydrogen halides, and hydrogen sulfide. *J. Org. Chem.*, **1967**, *32*, 2470-2472. DOI: 10.1021/jo01283a025
- 42. Kono, H.; Ojima, I.; Matsumoto, M.; Nagai, Y. A Convenient Route to Aminosilanes Using Hydrosilane-Rhodium(I) Complex Combinations. *Org. Prep. Proced. Int.* **1973**, *5*, 135-139. DOI: 10.1080/00304947309355562
- 43. Anrianov, K. A.; Filimonova, M. I.; Sidorov, V. I. Hydrosilylation of aromatic azomethins: I. Interconversion of final and intermediate compounds in the process of catalytic reaction of trialkyl- or aryl-hydrosilanes with benzylidene aniline. *J. Organomet. Chem.* **1977**, *142*, 31-37. DOI: 10.1016/S0022-328X(00)91813-8

- 44. Biran, C.; Blum, Y. D.; Glaser, R.; Tse, D. S.; Youngdahl, K. A.; Laine. R. M. Catalytic synthesis of oligosilazanes part 2. *J. Mol. Catal.*, **1988**, *48*, 183-197. DOI: 10.1016/0304-5102(88)85004-1
- 45. Matarasso-Tchiroukhine, E. AreneCr(CO)₂(η²-HSiHPh₂) complexes as catalysts for the Si–H bond activation. Hydrolysis of the Si–H bond and dehydrogenative coupling between diphenylsilane and nucleophiles. *J. Chem. Soc., Chem. Commun.*, **1990**, 681-682. DOI: 10.1039/C39900000681
- 46. Tsuchimoto, T.; Iketani Y.; Sekine, M. Zinc-Catalyzed Dehydrogenative N-Silylation of Indoles with Hydrosilanes. *Chem. Eur. J.*, **2012**, *18*, 9500-9504. DOI: 10.1002/chem.201200651 47. Königs, C. D. F.; Müller, M. F.; Aiguabella, N.; Klare, H. F. T.; Oestreich, M. Catalytic dehydrogenative Si-N coupling of pyrroles, indoles, carbazoles as well as anilines with hydrosilanes without added base. *Chem. Commun.*, **2013**, *49*, 1506-1508. DOI: 10.1039/C3CC38900F
- 48. Yonekura, K.; Iketani, Y.; Sekine, M.; Tani, T.; Matsui, F.; Kamakura, D.; Tsuchimoto, T. Zinc-Catalyzed Dehydrogenative Silylation of Indoles. *Organometallics*, **2017**, *36*, 3234-3249. DOI: 10.1021/acs.organomet.7b00382
- 49. Rios, P.; Rosello-Merino, M.; Rivada-Wheelaghan, O.; Borge, J.; Lopez-Serrano, J.; Conejero, S. Selective catalytic synthesis of amino-silanes at part-per million catalyst loadings. *Chem. Commun.*, **2018**, *54*, 619-622. DOI: 10.1039/C7CC08530C
- 50. Zhai, W.; Li, B.; Wang, B. Ru₃(CO)₁₂-catalyzed dehydrogenative Si–N coupling of indoles with hydrosilanes without additive. *Tetrahedron*, **2018**, *74*, 1123-1128. DOI: 10.1016/j.tet.2018.01.024
- 51. Reuter, M. B.; Cibuzar, M. P.; Hammerton, J.; Waterman, R. Photoactivated silicon—oxygen and silicon—nitrogen heterodehydrocoupling with a commercially available iron compound. *Dalton Trans.*, **2020**, *49*, 2972-2978. DOI: 10.1039/C9DT04870G
- 52. Takaki, K.; Kamata, T.; Miura, Y.; Shishido, T.; Takehira, K. Dehydrogenative Silylation of Amines and Hydrosilylation of Imines Catalyzed by Ytterbium–Imine Complexes. *J. Org. Chem.*, **1999**, *64*, 3891-3895. DOI: 10.1021/jo982154r
- 53. Wang, J. X.; Dash, A. K.; Berthet, J. C.; Ephritikhine, M.; Eisen, M. S. Dehydrocoupling reactions of amines with silanes catalyzed by [(Et₂N)₃U][BPh₄], *J. Organomet. Chem.*, **2000**, *610*, 49-57. DOI: 10.1016/S0022-328X(00)00410-1

- 54. Xie, W.; Hu, H.; Cui, C. [(NHC)Yb{N(SiMe₃)₂}₂]-Catalyzed Cross-Dehydrogenative Coupling of Silanes with Amines. *Angew. Chem. Int. Ed.*, **2012**, *51*, 11141-11144. DOI: 10.1002/ange.201205317
- 55. Pindwal, A.; Ellern, A.; Sadow, A. D. Homoleptic Divalent Dialkyl Lanthanide-Catalyzed Cross-Dehydrocoupling of Silanes and Amines. *Organometallics*, **2016**, *35*, 1674-1683. DOI: 10.1021/acs.organomet.6b00138
- 56. Cibuzar, M. P.; Waterman, R. Si–N Heterodehydrocoupling with a Lanthanide Compound. *Organometallics*, **2018**, *37*, 4395-4401. DOI: 10.1021/acs.organomet.8b00372
- 57. Zhang, X.; Zhou, S.; Fang, X.,; Zhang, L.; Tao, G.; Wei, Y.; Zhu, X.; Cui, P.; Wang, S. Syntheses of Dianionic α-Iminopyridine Rare-Earth Metal Complexes and Their Catalytic Acitivities toward Dehydrogenative Coupling of Amines with Hydrosilanes. *Inorg. Chem.*, **2020**, *59*, 9683-9692. DOI: 10.1021/acs.inorgchem.0c00907
- 58. Rina Y. A.; Schmidt, J. A. R. Heterodehydrocoupling of Silanes and Amines Catalyzed by a Simple Lanthanum-Based Complex. *Organometallics*, **2022**, *41*, 2974-2984. DOI: 10.1021/acs.organomet.2c00404
- 59. Leland, B.; Mondal, J.; Trovitch, R. J. Sustainable preparation of aminosilane monomers, oligomers, and polymers through Si–N dehydrocoupling catalysis. *Chem. Commun.* **2023**, *59*, 3665-3684. DOI:10.1039/d2cc07092h.
- 60. Sharma, A.; So, S.; Kim, J.-H.; MacMillan, S. N.; Baik, M.-H.; Trovitch, R. J. An aryl diimine cobalt(I) catalyst for carbonyl hydrosilylation. *Chem. Commun.* **2022**, *58*, 10793-10796. DOI: 10.1039/D2CC04089A
- 61. Batha, H. D.; Whitney, E. D. Kinetics and Mechanism of the Thermal Decomposition of Si₃N₄. *J. Am. Ceram. Soc.* **1973**, *56*, 365-369. DOI: 10.1111/j.1151-2916.1973.tb12687.x
- 62. Sarin, V. K. On the α-to-β phase transformation in silicon nitride. *Mat. Sci. Eng. A*, **1988**, *105-106*, 151-159. DOI: 10.1016/0025-5416(88)90491-0
- 63. Laine, R. M.; Blum, Y. D.; Hamlin, R. D.; Chow, A. In Ultrastructure Processing of Ceramics, Glasses and Composites II, Ed. Mackenzie, D. J.; Ulrich, D. R. John Wiley & Sons, New York, **1988**, pp. 761-769.
- 64. Kozuch, S.; Martin, J. M. L. "Turning Over" Definitions in Catalytic Cycles. *ACS Catal.* **2012**, *2*, 2787-2794. DOI: 10.1021/cs3005264

65. Fricke, J.; Heinemann, U.; Ebert, H. P. Vacuum insulation panels—From research to market. *Vacuum*, **2008**, *82*, 680-690. DOI: 10.1016/j.vacuum.2007.10.014

66. Li, W.; Chung, H.; Daeffler, C.; Johnson, A. J.; Grubbs, R. H. Application of ¹H DOSY for Facile Measurement of Polymer Molecular Weights. *Macromolecules*, **2012**, *45*, 9595-9603.

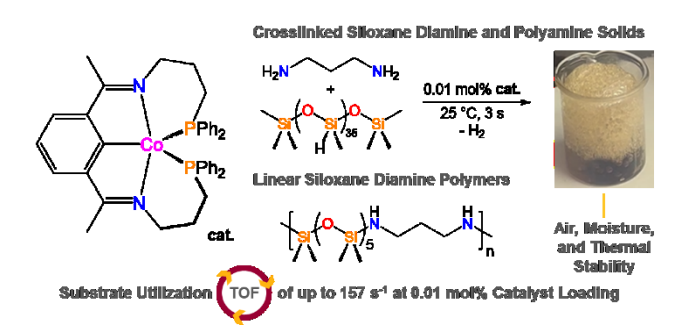
DOI: 10.1021/ma301666x

67. Okada, M. Chemical syntheses of biodegradable polymers. *Prog. Polym. Sci.*, **2002**, 27, 87-133. DOI: 10.1016/S0079-6700(01)00039-9

68. Schneiderman, D. K.; Hillmyer, M. A. 50th Anniversary Perspective: There Is a Great Future in Sustainable Polymers. *Macromolecules*, **2017**, *50*, 3733-3749. DOI:

10.1021/acs.macromol.7b00293

TOC GRAPHIC



SYNOPSIS

The dehydrocoupling of diamines and polyamines to hydride-functionalized siloxanes has been achieved with substrate utilization turnover frequencies of up to 157 s⁻¹ at ambient temperature.